Energy Proceedings
Vol 53, 2025
ISSN 2004-2965

The Energy Supply Capacity of Integrated Energy Systems#

Tianshuo Zhou[1], Dan Wang[1,2*], Hongjie Jia[1,2], Shuai Zhang[1]

1 Key Laboratory of the Ministry of Education on Smart Power Grids (Tianjin University), Tianjin 300072, China

2 Key Laboratory of Smart Energy & Information Technology of Tianjin Municipality (Tianjin University), Tianjin 300072, China

(Corresponding Author: wangdantjuee@tju.edu.cn)

ABSTRACT

Safety analysis is an essential tool for ensuring the economic and stable operation of integrated energy systems and is a crucial component of the energy management system. Given that the security region of tightly coupled electric-gas-heat integrated energy systems has not been extensively studied, this paper establishes the security region model and the total energy supply capability model for the integrated energy system. It discusses and analyzes the total energy supply capability and security region characteristics of the tightly coupled electric-gas-heat integrated energy system, highlighting the impact of coupling nodes on the thermal system's heating capacity and the relationship between the total energy supply capability and load size.

Keywords: security region, Integrated Energy Systems, Total Energy Supply Capability, security boundary

NONMENCLATURE

Abbreviations	
IES	Integrated Energy Systems
SR	Security Region
TEnSC	Total Energy Supply Capability
$TEnSC_{max}$	Maximum value of TEnSC
$TEnSC_{min}$	Minimum value of TEnSC
CHP	Combined Heat and Power
CP	Circulating water Pump
Symbols	
$\boldsymbol{W}_S$	Operating point vector
$\boldsymbol{\Omega}_{SR}$	Security Region

1. INTRODUCTION

Due to the differences in structure, characteristics, and composition of various energy subsystems, the coupling forms are diverse and complex, presenting new challenges for the safe operation of IES. In terms of static security analysis of IES, although existing research has established security region(SR)[1-2] model, the security analysis of tightly coupled electricity-gas-heat integrated energy systems has not yet been explicitly studied.

Therefore, this paper first establishes a security region model and a maximum energy supply capacity model for IES. Based on a case study of a tightly coupled electricity-gas-heat IES, it discusses and analyzes the energy supply capacity and security region characteristics of such systems.

2. MODEL FOR SECURITY ANALYSIS

2.1 Security region model of IES

This paper approaches the issue from the perspective of the maximum output of IES operation, without considering N-1 contingency factors, and focuses on the impact of multi-energy flows on system operation under the N-0 security criterion.

2.1.1 Definition of Operational point

The operating point is defined as the minimal set of state variables that characterize system security under normal operating conditions. Assuming an IES contains several load nodes, the operating point can be represented as a vector in Euclidean space:

$$\boldsymbol{W}_S = \begin{bmatrix} P_{H1}, P_{H2}, \ldots, P_{Hi}, \ldots P_{Hm}, \\ P_{E1}, P_{E2}, \ldots, P_{Ej}, \ldots P_{En}, \\ m_{GQ1}, m_{GQ2}, \ldots, m_{GQk}, \ldots m_{GQo}, \end{bmatrix} \quad (1)$$

In the formula: $\boldsymbol{W}_S$ represents the operating point vector. P_{Hi} represents the thermal load power at the *i*-th thermal node. P_{Ej} represents the electrical load power at the *j*-th electrical node. m_{GQk} represents the gas load flow at the *k*-th gas node. *m* is the highest index of the thermal load nodes (excluding coupling nodes). *n* is the highest index of the electrical load nodes (excluding coupling nodes). *o* is the highest index of the gas load nodes (excluding coupling nodes).

This is a paper for the 16th International Conference on Applied Energy (ICAE2024), Sep. 1-5, 2024, Niigata, Japan.

2.1.2 Definition of N-0 Security region

The security region in an IES is defined as the set of all operating points $P(m)$ that satisfy the safety operational constraints, including energy balance constraints, energy network constraints, and coupling equipment output constraints. If an operating point lies within the security region, it satisfies all operational constraints and can be considered as operating safely or N-0 safe. Conversely, if it lies outside the security region, it is considered unsafe.

2.1.3 Security region model

The mathematical general form for constructing the security region model of an IES can be expressed as:

$$\boldsymbol{\Omega}_{\mathrm{SR}}=\left\{\boldsymbol{W}_{\mathrm{S}} \mid h\left(\boldsymbol{W}_{\mathrm{S}}\right)=0,\ g\left(\boldsymbol{W}_{\mathrm{S}}\right) \leq 0\right\} \tag{2}$$

In the equation: $\boldsymbol{\Omega}_{\mathrm{SR}}$ denotes the security region. $h\left(\boldsymbol{W}_{\mathrm{S}}\right)=0$ is the set of equality constraints that the IES must satisfy for N-0 security, including power flow equality constraints, gas and thermal system energy flow equality constraints, and coupling node equality constraints. $g\left(\boldsymbol{W}_{\mathrm{S}}\right) \leq 0$ is the set of inequality constraints that the IES must satisfy for N-0 security.

The set of equality constraints can be referred to in the literature [1], and will not be elaborated here. $g\left(\boldsymbol{W}_{\mathrm{S}}\right) \leq 0$ include: Thermal system security operation inequality constraints $\boldsymbol{H}_{\mathrm{H}}$, Electrical system security operation inequality constraints $\boldsymbol{H}_{\mathrm{E}}$, Gas system security operation inequality constraints $\boldsymbol{H}_{\mathrm{G}}$, and Coupling node security operation inequality constraints $\boldsymbol{H}_{\mathrm{ES}}$. These are detailed as follows:

$$\begin{cases} g\left(\boldsymbol{W}_{\mathrm{S}}\right)=\left\{\boldsymbol{H}_{\mathrm{H}}, \boldsymbol{H}_{\mathrm{E}}, \boldsymbol{H}_{\mathrm{G}}, \boldsymbol{H}_{\mathrm{ES}}\right\} \\ \boldsymbol{H}_{\mathrm{H}}=\begin{cases} \boldsymbol{T}_{\mathrm{s,min}} \leq \boldsymbol{T}_{\mathrm{s}} \leq \boldsymbol{T}_{\mathrm{s,max}} \\ \boldsymbol{T}_{\mathrm{r,min}} \leq \boldsymbol{T}_{\mathrm{r}} \leq \boldsymbol{T}_{\mathrm{r,max}} \\ \boldsymbol{m}_{\mathrm{H,min}} \leq \boldsymbol{m}_{\mathrm{H}} \leq \boldsymbol{m}_{\mathrm{H,max}} \end{cases} \\ \boldsymbol{H}_{\mathrm{E}}=\begin{cases} \boldsymbol{v}_{\mathrm{am,min}} \leq \boldsymbol{v}_{\mathrm{am}} \leq \boldsymbol{v}_{\mathrm{am,max}} \\ \boldsymbol{\vartheta}_{\mathrm{E,min}} \leq \boldsymbol{\vartheta}_{\mathrm{E}} \leq \boldsymbol{\vartheta}_{\mathrm{E,max}} \\ 0 \leq \boldsymbol{p}_{\mathrm{E}} \leq \boldsymbol{p}_{\mathrm{E,max}} \\ 0 \leq \boldsymbol{p}_{\mathrm{Eg}} \leq \boldsymbol{p}_{\mathrm{Eg,max}} \end{cases} \\ \boldsymbol{H}_{\mathrm{G}}=\begin{cases} \boldsymbol{p}_{\mathrm{GP,min}} \leq \boldsymbol{p}_{\mathrm{GP}} \leq \boldsymbol{p}_{\mathrm{GP,max}} \\ \boldsymbol{m}_{\mathrm{GL,min}} \leq \boldsymbol{m}_{\mathrm{GL}} \leq \boldsymbol{m}_{\mathrm{GL,max}} \\ \boldsymbol{m}_{\mathrm{GQ,min}} \leq \boldsymbol{m}_{\mathrm{GQ}} \leq \boldsymbol{m}_{\mathrm{GQ,max}} \end{cases} \\ \boldsymbol{H}_{\mathrm{ES}}=\begin{cases} \boldsymbol{P}_{\mathrm{HP}} \leq \min\left(\boldsymbol{CHP}_{\mathrm{E}}, \boldsymbol{C}_{\mathrm{HP}}\right) \\ \boldsymbol{CHP}_{\mathrm{E}} \leq \boldsymbol{C}_{\mathrm{CHP,E}} \\ \boldsymbol{CHP}_{\mathrm{H}} \leq \boldsymbol{C}_{\mathrm{CHP,H}} \end{cases} \end{cases} \tag{3}$$

In the formula: $\boldsymbol{T}_{\mathrm{s}}$ is the column vector of supply water temperatures at thermal nodes; $\boldsymbol{T}_{\mathrm{s,max}}$ and $\boldsymbol{T}_{\mathrm{s,min}}$ are column vectors representing the upper and lower limits of $\boldsymbol{T}_{\mathrm{s}}$, respectively. $\boldsymbol{T}_{\mathrm{r}}$ is the column vector of return water temperatures at thermal nodes; $\boldsymbol{T}_{\mathrm{r,max}}$ and $\boldsymbol{T}_{\mathrm{r,min}}$ are column vectors representing the upper and lower limits of $\boldsymbol{T}_{\mathrm{r}}$, respectively. $\boldsymbol{m}_{\mathrm{H}}$ is the column vector of flow rates in thermal pipelines; $\boldsymbol{m}_{\mathrm{H,max}}$ and $\boldsymbol{m}_{\mathrm{H,min}}$ are column vectors representing the upper and lower limits of $\boldsymbol{m}_{\mathrm{H}}$, respectively. $\boldsymbol{v}_{\mathrm{am}}$ is the column vector of voltage magnitudes at power system nodes; $\boldsymbol{v}_{\mathrm{am,max}}$ and $\boldsymbol{v}_{\mathrm{am,min}}$ are column vectors representing the upper and lower limits of $\boldsymbol{v}_{\mathrm{am}}$, respectively. $\boldsymbol{\vartheta}_{\mathrm{E}}$ is the column vector of phase angle differences in power system branches; $\boldsymbol{\vartheta}_{\mathrm{E,max}}$ and $\boldsymbol{\vartheta}_{\mathrm{E,min}}$ are column vectors representing the upper and lower limits of $\boldsymbol{\vartheta}_{\mathrm{E}}$, respectively. $\boldsymbol{p}_{\mathrm{E}}$ is the distribution matrix of active power flows in power system branches; $\boldsymbol{p}_{\mathrm{E,max}}$ is the upper limit distribution matrix of $\boldsymbol{p}_{\mathrm{E}}$. $\boldsymbol{p}_{\mathrm{Eg}}$ is the distribution matrix of power injections at power system generator nodes; $\boldsymbol{p}_{\mathrm{Eg,max}}$ is the upper limit distribution matrix of $\boldsymbol{p}_{\mathrm{Eg}}$. $\boldsymbol{p}_{\mathrm{GP}}$ is the column vector of gas pressures at nodes in the natural gas system; $\boldsymbol{p}_{\mathrm{GP,max}}$ and $\boldsymbol{p}_{\mathrm{GP,min}}$ are the column vectors representing the upper and lower limits of $\boldsymbol{p}_{\mathrm{GP}}$, respectively. $\boldsymbol{m}_{\mathrm{GL}}$ is the column vector of gas flow rates in the natural gas system pipelines; $\boldsymbol{m}_{\mathrm{GL,max}}$ and $\boldsymbol{m}_{\mathrm{GL,min}}$ are the column vectors representing the upper and lower limits of $\boldsymbol{m}_{\mathrm{GL}}$, respectively. $\boldsymbol{m}_{\mathrm{GQ}}$ is the column vector of gas flow rates at nodes in the natural gas system; $\boldsymbol{m}_{\mathrm{GQ,max}}$ and $\boldsymbol{m}_{\mathrm{GQ,min}}$ are the column vectors representing the upper and lower limits of $\boldsymbol{m}_{\mathrm{GQ}}$, respectively. $\boldsymbol{P}_{\mathrm{HP}}$ is the column vector of electric power of the circulating water pumps. $\boldsymbol{C}_{\mathrm{HP}}$ is the column vector of rated electric power of the circulating water pumps. $\boldsymbol{CHP}_{\mathrm{E}}$ and $\boldsymbol{CHP}_{\mathrm{H}}$ are the column vectors of electric power output and thermal power output of the CHP units, respectively; $\boldsymbol{C}_{\mathrm{CHP,E}}$ and $\boldsymbol{C}_{\mathrm{CHP,H}}$ are the column vectors of rated electric power output and rated thermal power output of the CHP units, respectively.

2.2 TEnSC model

All operating points within the safety region are considered safe operating points. To enhance the economic efficiency of system operation, and to further

explore the system's energy supply capacity limits while ensuring safe operation, the maximum total energy supply capacity index of the IES, denoted as $TEnSC_{max}$, is introduced. This index is defined as the maximum energy supply capacity to multi-energy loads under the constraints of the safety region model. Therefore, the calculation of the $TEnSC_{max}$ index essentially involves solving an optimization model that aims to maximize the total energy supply to multi-energy loads within the system, with the safety region model serving as the constraint. This can be specifically expressed as follows:

$$\begin{cases} \mathrm{TEnSC}_{\max} = \max\left(\sum_{i}^{m} P_{Hi} + \sum_{j}^{n} P_{Ej} + \sum_{k}^{o}\left(\frac{1000}{3600}\cdot m_{\mathrm{GQ}k}\cdot \mathrm{GCV}\right)\right) \quad (3) \\ \text{s.t.} \quad h(\boldsymbol{W}_{\mathrm{S}})=0 \\ \qquad g(\boldsymbol{W}_{\mathrm{S}})\le 0 \end{cases}$$

In the formula: $TEnSC_{max}$ represents the maximum energy supply capacity limit of the IES. GCV is the calorific value of natural gas, taken as 45.574 MJ/m³.

Reference [1] constructs operating points based on source-side output and calculates the TEnSC, including network losses. In contrast, this paper constructs operating points based on load-side power and calculates the TEnSC from these points. Compared to Reference [1], this paper aims to maximize the energy actually received by users, excluding internal system losses, resulting in a more accurate determination of the TEnSC.

2.3 Solution process

Based on the aforementioned theory and model, this paper first determines the $TEnSC_{max}$ operating point. Then, using simulation methods[3], it solves for the TEnSC curve and the safety region near the $TEnSC_{max}$ operating point. Specifically, this includes three steps: calculating and solving for $TEnSC_{max,}$ deriving the TEnSC curve, and characterizing the safety region.

1) Calculation and Solution of $TEnSC_{max}$. The system's $TEnSC_{max}$ is set as the optimization objective, with the IES safety region model as the constraint. The barrier function interior point method is employed to solve for the system's $TEnSC_{max}$ operating point, obtaining the distribution of electric power, thermal power, and gas flow when the total load of the network reaches the $TEnSC_{max}$ operating point.
2) TEnSC Curve. Take the load node P_{Hi} (or P_{Ej}、m_{GQk}) as the observation node and treat it as a free variable, while the remaining load nodes correspond to the power or flow at the TEnSCmax operating point. Let the parameter of the observation node take values from its lower limit to its upper limit in increments of ΔP_{H}, obtaining several operating points. Substitute each operating point into the calculations from step 1) to determine the corresponding TEnSC values. If the safety constraints are satisfied, record these values into the safe operating point array. Repeat the above steps, traversing all load nodes to obtain a complete array of safe operating points. Sort the safe operating points in ascending order according to their TEnSC values to obtain the sampling points. Plot the TEnSC curve using the sample point indices as the x-axis and the TEnSC values of the sampling points as the y-axis.
3) Characterization of the Safety Region. Select load nodes (H_m, E_n, G_o) as observation nodes and treat the power/flow combinations (P_{Hm}, P_{En}, m_{Go}) of the observation nodes as free variables, where P_{Hm}, P_{En} and m_{Go} represent the thermal power, electric power, and flow of load nodes H_m, E_n and G_o, respectively. The loads of the other nodes correspond to the values at the $TEnSC_{max}$ operating point, and the power of all load nodes are also treated as free variables. Let P_{Hm}, P_{En} and m_{Go} incrementally approach their upper limits from their lower limits in steps of ΔP_{H}, ΔP_{E}, and ΔP_{G}, respectively, to obtain several operating point combinations. Substitute these combinations into the calculations from step 1) to perform safety checks on each operating point. If an operating point passes the safety check, record it as a safe operating point; if it fails, record it as an unsafe operating point. Use P_{Hm}, P_{En}, and m_{Go} as coordinate axes and plot a 3D safety region and state space using the TEnSC values of the various operating points as data.

3. CASE STUDY

3.1 Introduction to case

The example consists of a 4-node power system, a 5-node natural gas system, and a 3-node thermal system. The parameter ranges for each system are shown in Tables 1- Tables 6. Nodes E_3, H_3, and G_5 are coupled by a Combined Heat and Power (CHP) unit, with a CHP heat-to-power ratio of 1.3 and a CHP natural gas distribution coefficient of 0.5. The rated power of the circulating water pump (CP) is 0.3 MW. The calorific value of natural gas is 45.574 MJ/m³, and the theoretical combustion temperature is 1973 ℃. Detailed parameters of the thermal system can be found in reference [4].

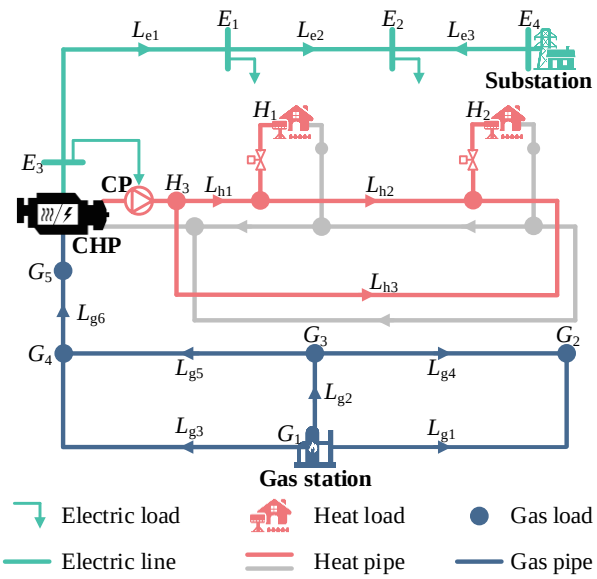

Fig. 1 diagram of case

Table 1 The node parameters of power system

Node	Node type	Voltage amplitude range(p.u.)	Active power range of the source(MW)	Load power range(MWA)
E_1	PQ nodes	[0.95, 1.05]	-	[0.1053, 1.26]
E_2	PQ nodes	[0.95, 1.05]	-	[0.1053, 1.26]
E_3	PV nodes	1.05	[0, 5]	-
E_4	Balance nodes	1.02	[0, 5.5385]	-

Table 2 The branch parameters of power system

No.	First node	End node	Impedance(p.u.)	Line capacity(MWA)
L_{e1}	E_3	E_1	0.09+j0.1577	5.83
L_{e2}	E_1	E_2	0.09+j0.1577	5.83
L_{e3}	E_4	E_2	0.09+j0.1577	5.83

Table 3 The node parameters of gas system

Node	Node type	Pressure range (mbar)
G_1	Source	[75, 75]
G_2	Load	[22.5, 75][5]
G_3	Load	[22.5, 75][5]
G_4	Load	[22.5, 75][5]
G_5	Load	[22.5, 75][5]

Table 4 The branch parameters of gas system

No.	First node	End node	Flow range (m^3/h)	Length (m)	diameter (mm)
L_{g1}	G_1	G_2	[0, 394.12]	280	150
L_{g2}	G_1	G_3	[0, 394.12]	300	100
L_{g3}	G_1	G_4	[0, 394.12]	220	100
L_{g4}	G_3	G_2	[0, 394.12]	300	100
L_{g5}	G_3	G_4	[0, 394.12]	240	100
L_{g6}	G_4	G_5	[0, 394.12]	200	100

Table 5 The node parameters of heat system

Node	Node type	Supply temp. (℃)	Return temp. (℃)	Thermal power (MW_{th})
H_1	Load	[95, 100]	[45, 50]	[0.01, 5]
H_2	Load	[95, 100]	[45, 50]	[0.01, 5]
H_3	Source	[100, 100]	[45, 50]	[-5, 0]

Table 6 The branch parameters of heat system

No.	First node	End node	Flow range (kg/s)	Length (m)	diameter (mm)
L_{h1}	H_3	H_1	[0, 23.91]	400	150
L_{h2}	H_1	H_2	[0, 23.91]	400	150
L_{h3}	H_3	H_2	[0, 23.91]	600	150

3.2 Results

Using the barrier function interior point method, the $TEnSC_{max}$ of the IES is calculated to be 13.6816 MW. The load distribution at the $TEnSC_{max}$ operating point is shown in the table 7. The red values correspond to the results of the balance nodes or coupling nodes.

Table 7 Power distribution at $TEnSC_{max}$

Type	Load	End node	
E_1	0.9103 MW	G_3	394.1200 m^3/h
E_2	0.4965 MW	G_4	394.1200 m^3/h
E_3	-0.5460 MW	G_5	172.5179 m^3/h
E_4	-1.0059 MW	H_1	0.5470 MW
G_1	-1088.4051 m^3/h	H_2	0.1332 MW
G_2	127.6473 m^3/h	H_3	-0.7164 MW

Based on the TEnSCmax operating point and following the steps outlined in step 2), the TEnSC curve is plotted as shown in Figure 2. Under the condition of meeting safety constraints, the maximum energy supply capacity, TEnSCmax, is 13.6816 MW, and the minimum energy supply capacity, TEnSCmin, is 8.3423 MW. This delineates the energy supply capacity range of the IES, providing a valuable reference for dispatch operators.

Further, according to step 3), the active power combinations (P_{E1}, P_{E2}) at the load nodes E_1 and E_2 of the power system are selected as free variables for two-dimensional observation, with the remaining load nodes at the values corresponding to the $TEnSC_{max}$ operating point. The active power combinations (P_{E1}, P_{E2}) increment by 0.05 MW from the lower limit to the upper limit of the power node loads, generating 529 operating points. Multi-energy flow calculations are performed on each operating point to analyze safety. As shown in the figure 3, the state space of the operating points is depicted by the blue dashed line, and the safety region is depicted by the red dash-dot line.

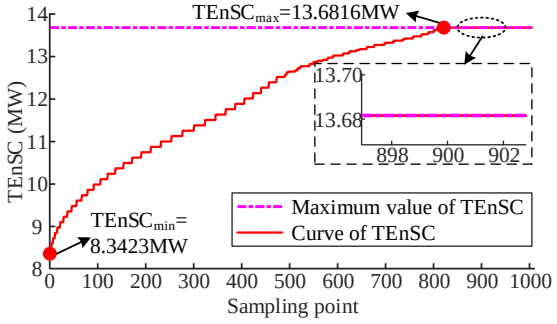

Fig. 2 Curve of the TEnSC

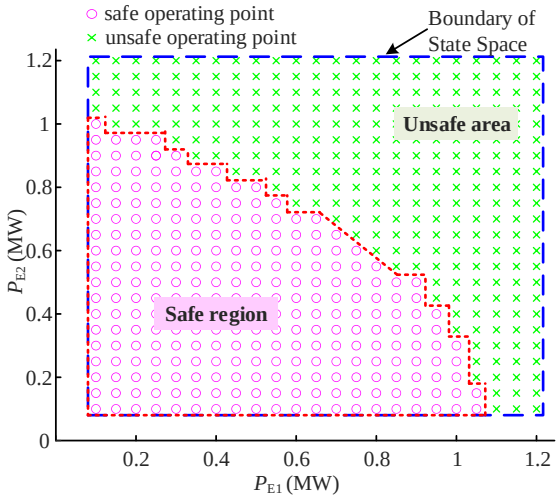

Fig. 3 Two-dimensional security region based on (P_{E1}, P_{E2})

Similarly, the gas flow rate combinations (m_{G2}, m_{G3}) at the load nodes G_2 and G_3 of the natural gas system are selected as free variables for two-dimensional observation, with the remaining load nodes at the values corresponding to the $TEnSC_{max}$ operating point. The gas flow rate combinations (m_{G2}, m_{G3}) increment by 15 m³/h from the lower limit to the upper limit of the gas load, generating 529 operating points. Multi-energy flow calculations are performed on each operating point to analyze safety. As shown in Figure 4, the state space of the operating points is depicted by the orange dashed line, and the safety region is depicted by the light blue dash-dot line.

The thermal power combinations (P_{H1}, P_{H2}) at the load nodes H_1 and H_2 of the thermal system are selected as free variables for two-dimensional observation, with the remaining load nodes at the values corresponding to the $TEnSC_{max}$ operating point. The thermal power combinations (P_{H1}, P_{H2}) increment by 10^{-4} kW, with the thermal load H_1 ranging from [546.9896 kW to 546.9919 kW] and the thermal load H_2 ranging from [133.2165 kW to 133.2185 kW], generating 442 operating points. Multi-energy flow calculations are performed on each operating point to analyze safety. As shown in the figure 5, the state space of the operating points is depicted by the black dashed line, and the safety region is depicted by the green dash-dot line.

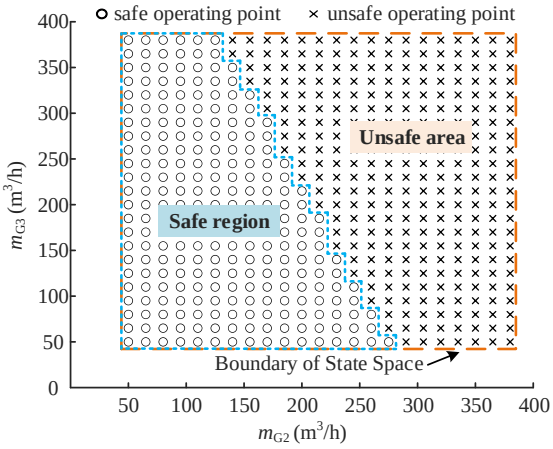

Fig. 4 Two-dimensional security region based on (m_{G2}, m_{G3})

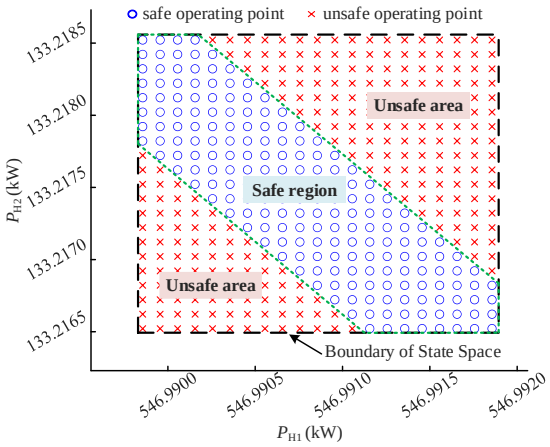

Fig. 5 Two-dimensional security region based on (P_{H1}, P_{H2})

It is worth noting that the range of values for the thermal load is very narrow. This is due to constraints imposed by the coupling nodes in the thermal system, such as the gas pressure constraint at gas node G_5, the gas flow constraints in pipelines L_{g1}-L_{g6}, and the voltage constraint at power node E_3. Specifically, reducing the thermal load tends to cause the voltage at power node E_3 to fall below its lower limit, while increasing the thermal load tends to cause the gas flow in pipelines L_{g1}-L_{g6} to exceed its upper limit and the gas pressure at gas node G_5 to fall below its lower limit.

The thermal load node H_1, the power load node E_2, and the gas load node G_2 are selected to form the combination (P_{H1}, P_{E1}, m_{G2}) as free variables for three-dimensional observation, with the remaining load nodes at the values corresponding to the $TEnSC_{max}$ operating point. The step size follows the same approach as

previously described, generating 5796 operating points. Multi-energy flow calculations are performed on each operating point to test for safety. As shown in Figure 6, the three-dimensional state space of the operating points is depicted by the blue dashed line, and the three-dimensional safety region is depicted by the red solid line, forming a hexahedron. When the combination is (546.9918 kW, 0.9 MW, 125 m³/h), the system reaches $TEnSC_{max}$. When the combination is (546.9900 kW, 0.1 MW, 50 m³/h), the system reaches $TEnSC_{min}$.

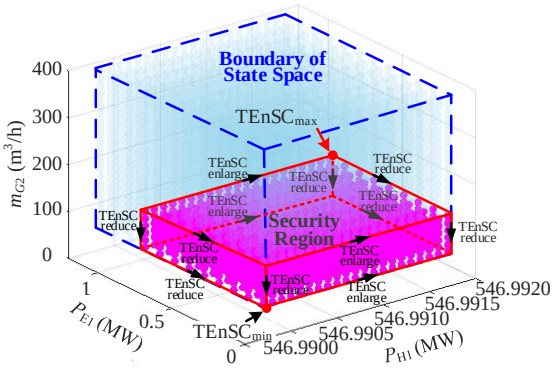

Fig. 6 Three-dimensional security region based on (P_{H1}, P_{E1}, m_{G2})

From the three-dimensional safety region, it can be observed that an increase in the load at thermal load node H_1 leads to an increase in TEnSC value; a decrease in the load at power load node E_1 leads to a decrease in TEnSC value, and a decrease in the load at gas load node G_2 also leads to a decrease in TEnSC value. Therefore, it can be concluded that, in this case, TEnSC value exhibits a positive correlation with each of the loads.

4. CONCLUSIONS

This paper establishes a maximum energy supply capacity model and a safety region model for an IES with close coupling of electricity, gas, and heat. The effectiveness of the model is validated using a typical example. The specific conclusions are as follows:

1) The upper and lower limits of the energy supply capacity and the safety region of the IES are characterized, guiding dispatch operators to avoid unsafe operating conditions as much as possible. Compared to Reference [1], this paper aims to maximize the energy actually received by users, excluding internal system losses, resulting in a more accurate determination of the TEnSC.
2) In an IES with CHP as the coupling element, the thermal system is influenced by gas pressure constraints and flow constraints of the natural gas system, as well as voltage constraints of the power system. Under the premise of ensuring the safe operation of the IES, the load variation range of thermal nodes is very small, indicating a limited adjustable range of heating capacity.
3) Under the premise of the safe operation of the IES, TEnSC value exhibits a positive correlation with each of the loads

ACKNOWLEDGEMENT

This work was supported by National Natural Science Foundation of China (No. 51977141), National Key R&D Program of China (No. 2018YFB0905000), Science and Technology Project of SGCC (No. SGTJDK00DWJS1800232). This study was conducted in cooperation of APPLIED ENERGY UNiLAB-DEM: Distributed Energy & Microgrid. UNiLAB is an international virtual lab of collective intelligence in Applied Energy.

REFERENCE

[1] LIU Liu, WANG Dan, JIA Hongjie, et al. Operation region model for integrated energy distribution system[J]. Eleetri Power Automation Equipments, 2019, 39(10): 1-9.

[2] LIU Liu, WANG Dan, HOU Kai, et al. Region model and application of regional integrated energy system security analysis[J]. Applied Energy, 2019, 260: 114268.

[3] Ding Lei, Gonzalez-Longatt F M, Wall P,et al. Two-Step Spectral Clustering Controlled Islanding Algorithm[J]. IEEE Transactions on Power Systems, 2013, 28(1):75-84.

[4] ZHOU Tianshuo, WANG Dan, JIA Hongjie. Energy and Exergy State Estimation Methods for Integrated Energy Systems[J]. Eleetri Power Automation Equipments, 2024.

[5] WANG Weiliang, WANG Dan, JIA Hongjie, et al. Analysis of Energy Flow Optimization in Regional Electricity-Gas-Heat Integrated Energy System Considering Operational Constraints[J]. Proceedings of the CSEE, 2017, 37(24): 7108-7120.